Potential Anticancer Agents: Exploring the Cytotoxic Effects of Tetramine-Based Schiff Bases on MDA-MB-231 Breast Cancer Cells

G.M. Hemalatha [a]*, R. Epshiba[b], *Kandasamy Thirunavukkarasu*[c]*

[a]*Mohan Babu University, Tirupathi-517102, Andhra Pradesh, India.*

[b]*S.A. Engineering College, Chennai -600077, India.*

[c]*Vel Tech Rangarajan Dr. Sagunthala R&D Institute of Science and Technology,*

Chennai-600062, India.

Abstract:

Three biphenyl-3,4,3',4'-tetraamine-based Schiff bases, L1, L2, and L3, derived from 2-thiophene carbaldehyde, 2-furaldehyde, and indole-3-carbaldehyde, respectively were successfully synthesized by simple reflexing by adding 1:4 ratio of the base tetraamine and the corresponding compounds for 6 hours. The synthesized compounds L1, L2 and L3 were characterized with ^{1}H NMR, ^{13}C NMR, FTIR, and mass spectrometry. The above compounds were tested in vitro for anti-cancer activity against MDA-MB-231 cell lines. Different concentrations of the compounds L1, L2 and L3, i.e., 5, 10, 15, 20, 25 and 30 µM were prepared and tested for the anticancer activities. Notably, studies for cell cytotoxicity (MTT assay) and apoptosis using acridine orange/ethidium bromide (AO/EB) dual staining revealed that the synthesized Schiff bases exhibited considerable anticancer activity. The results showed that the compounds L1, L2, and L3 displayed moderate anticancer activity and followed the order L2>L1>L3 with respect to IC_{50} values.

Keywords:

MDA-MB-231 cell lines, cytotoxicity, carcinoma, apoptosis assay, dual staining, MTT assay.

Introduction:

Cancer is currently one of the leading causes of death worldwide, according to the World Health Organization (WHO) cancer report released in 2024. *[1]*. According to the estimates, cancer accounts for one in six fatalities in the world. One in twelve women in countries with a very high Human Development Index (HDI) will be diagnosed with breast cancer in their lifetime, and a 1.4% mortality rate is found among those diagnosed [2]. The American Cancer Society (ACS) projected that in 2024, there would be approximately 2,001,140 new cancer cases and 611,720 cancer-related deaths in the United States, including an estimated 310,720 new cases of breast cancer in women and 42,250 associated deaths[3]. India is in third place after China and US in cancer deaths. According to GLOBOCAN, the number of cancer cases in India is projected to reach 2.08 million by 2040, representing a significant increase of 57.5% compared to 2020 *[4]*. Alarmingly, two-thirds of newly diagnosed cancer cases are already at an incurable stage. Additionally, the majority of cancer patients (over 60%) fall within the age range of 35 to 65 years [3].

Division and growth of cancer cells occur usually at a much faster rate than normal cells and naturally develop extreme stress *[5,6]*. Chemotherapeutic agents target cancer cells, halting their division and growth, and ultimately killing them. However, simultaneously, cancer cells develop resistance to these drugs, rendering them less effective over time *[7]*. The most common cancers are breast, rectum, lung, colon and prostate cancers. The development of cancer is influenced by a range of internal variables, including inherited mutations, hormonal factors, immunological conditions, and random mutations, in addition to various external factors, such as tobacco use, exposure to chemicals and radiation, and certain infectious agents *[8]*. Free radicals are formed when carcinogens enter our bodies, and they attempt to rob electrons from other molecules in the body. These free radicals harm cells and impair their capacity for regular activity *[9]*.

Breast cancer is the most common malignancy among women and one of the leading causes of death in females. *[10]* and it is a complicated disease *[11]*, which means that a wide range of events could lead to it. Since breast cancer was first documented by the ancient Egyptians more than 3500 years ago, it has a very lengthy history*[12,13]*. The majority of cancer-related deaths in women in the United States occur due to breast cancer, which is currently the second most common type of cancer *[14]*.

Approximately half of the cases of breast cancer occur in women without any known or established risk factors *[15]*. The illness is treated with surgery, chemotherapy, radiotherapy, and pharmaceuticals, but these methods have unfavourable side effects that reduce the patient's quality of life. Despite the fact that these treatments prolong lives, recurrence of the disease is common *[16]*. The side effects of chemotherapy that have been documented include neutropenia, nausea, vomiting, amenorrhea, alopecia, neurological damage, weight gain, secondary leukaemia, and cardiotoxicity*[17]*. Some of the side effects of hormone therapy include hot flashes, musculoskeletal pain, tiredness, mood fluctuations, nausea, vomiting, and fractures*[18]*. Precision medicine was formally introduced by the National Academy of Sciences in 2011. However, global research on breast cancer has accelerated dramatically since 2016*[19]*. Even though breast cancer cells like, MDA-MB-231, Hs578T, and BT-549 (triple negative breast cancer (TNBC) cells), SKBR3 (HER2+ breast cancer cell), MCF-7, T47D (Hormone Receptor-Positive (ER+/PR+) cells) are common, MDA-MB-231 is chosen because of the following reasons: i) MDA-MB-231 cell line is highly resistance against popular chemotherapy drugs like cisplatin[20] ii) they are highly invasive as well as metastatic[21] and iii) it is a triple negative breast cancer (TNBC) cell line [21].

Tetramines, particularly, spermine [22–24] plays an important role in the human metabolism and polyamines could be found in the urine of cancer patients [22]. Palladium complex of spermine was actually tested against triple negative breast cancer cell line, i.e., MDA-MB-231, which is highly resistant to cisplatin, most commonly used drug in chemotherapy, *in-vivo* in a xenograft mouse derived model [25] which gave promising results. The expensive spermine or spermine–Pd complex, an aliphatic tetramine, might be replaced with an inexpensive aromatic tetramine such as biphenyl-3,4,3',4'-tetraamine. Also, Schiff base with an azomethine –C=N functional group serves as the building block for numerous chemical compounds *[26–28]*. Hetero Schiff bases, in which a Schiff base is tied to the heterocyclic structures are of particular interest due to their special chelating characteristic brought on by the presence of electro negative atoms like N, O, and S donor atoms *[29–31]*. The biological activity of Schiff bases is one of the key fields of study, with the main objective being the identification of secure and efficient therapeutic agents for the treatment of bacterial infections and cancers *[32,33]*. Due to their low cost, ease of synthesis, and structural versatility, Schiff bases are widely utilized in various biological studies [34] and applications [35].

In this study, we synthesized, (N3Z, N4Z, N3'Z, N4'E)-N3, N3', N4, N4'-tetrakis (thiophen-2-ylmethylene) -[1,1'-biphenyl]-3, 3', 4, 4'-tetraamine (L1), (N3Z, N4Z, N3'Z, N4'E)-N3,N3',N4,N4'-tetrakis(furan-2-ylmethylene)-[1, 1'- biphenyl]-3, 3', 4, 4'-tetraamine (L2) and (N3E, N4Z, N3'Z, N4'E)-N3, N3', N4, N4'-tetrakis((1H-indol-2-yl)methylene)-[1,1'-biphenyl]-3,3',4,4'-tetraamine (L3). The structures were determined using a combination of analytical techniques, including ^{1}H NMR, ^{13}C NMR, mass spectrometry, and FT-IR spectroscopy. An MTT experiment was conducted to evaluate the IC_{50} values and cell morphologies as they are effective against breast cancer. AO/EB dual staining was performed with a fluorescence microscope at 20x magnification to identify cell apoptosis. The compounds that are made synthetically costs less and help breast cancer cells die. We as well studied the antibacterial and antifungal activities of the ligands, L1, L2 and L3 along with in-silico molecular docking studies and studied the binding affinities for the complex formation with Cu^{2+} and Zn^{2+} through DFT calculations.

Experimental:

Materials

All the solvents and chemicals like Biphenyl-3,4,3',4'-tetraamine, 2-thiophene carboxaldehyde, 2-furaldehyde, indole-3-carboxyaldehyde, nitrobenzene, DMSO, Streptomycin and bovine serum albumin used for the synthesis of compounds in the present work were purchased from Sigma Aldrich Chemicals Pvt. Ltd (India) and used without any further purification. Ethidium bromide (EB), Acridine orange (AO), 3-(4,5-dimethylthiozol-2-YI)-2,5-diphenyltetrazolium bromide (MTT), DMSO, PBS (phosphate buffered saline) (1%), Dulbecco`s Modified Eagle's Medium(DMEM),10% FBS (Fetal Bovine Serum), Penicillin-G used were of analytical grade, purchased from Hi media Laboratories Pvt. Ltd., India.

Methods

Synthesis of Schiff base L1 from biphenyl-3,4,3',4'-tetraamine and 2-thiophenecarboxyaldehyde:

The Schiff base (N3Z, N4Z, N3'Z, N4'E)-N3, N3', N4, N4'-tetrakis(thiophen-2-ylmethylene)-[1,1'-biphenyl]-3,3',4,4'-tetraamine) (L1) was synthesized from 1 mmol of biphenyl-3,4,3',4'-tetraamine and 4 mmol of 2-thiophenecarboxyaldehyde dissolved in 15 mL of a nitrobenzene and the reaction mixture solution was refluxed at 90^{o} C in an oil bath for 6 hrs with continuous stirring. Thin layer chromatography (TLC) was used to monitor the

course of the reaction. After completion of 6 hrs, the reaction mixture solution was cooled and transferred into the solvent hexane with continuous stirring. The raw product was completely purified by column chromatography and the major product was obtained as yellow solid. The yield was 85% (Table 1).

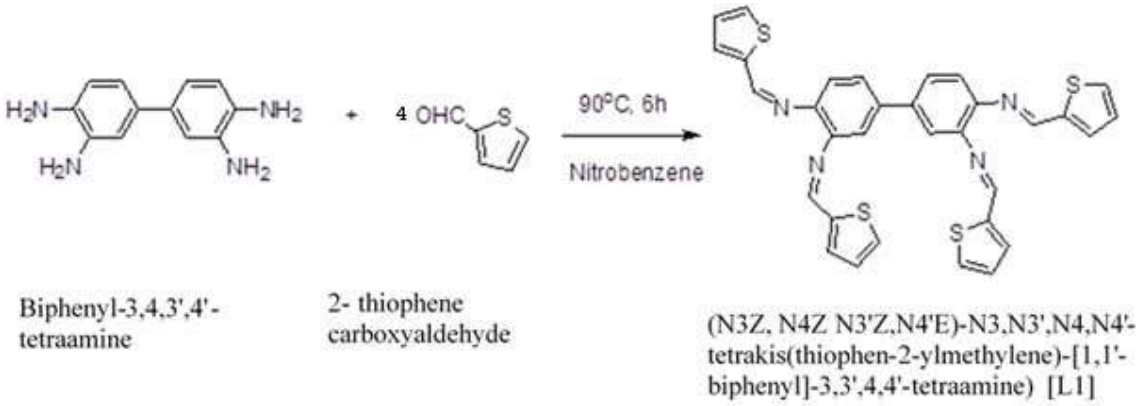

Scheme 1: Synthesis of N3Z, N4Z, N3'Z, N4'E)-N3, N3', N4, N4'-tetrakis(thiophen-2-ylmethylene)-[1,1'-biphenyl]-3,3',4,4'-tetraamine (L1) from biphenyl-3,4,3',4'-tetraamine and 2- thiophene carboxy aldehyde.

Table.1: Reaction conditions, Melting point and yield for the synthesis of Schiff bases L1, L2 and L3 from biphenyl-3,4,3',4'-tetraamine and 2-thiophenecarboxyaldehyde, 2-furaldehyde and Indole-3-carboxyaldehyde respectively.

Compound	Reaction Conditions		Melting Point, °C	Yield, %
	Temperature, °C	Time, h		
L1	RT	24	200	60
	90	6	200	85
L2	RT	24	165	65
	90	6	165	80
L3	RT	24	*Unable to purify	--
	90	6	~211	60

* Obtained several spots in TLC.

Synthesis of Schiff base L2 from biphenyl-3,4,3',4'-tetraamine and 2-furaldehyde:

The Schiff base (N3Z, N4Z, N3'Z, N4'E)-N3, N3', N4, N4'-tetrakis(furan-2-yl methylene)-[1,1'-biphenyl]-3,3',4,4'-tetraamine) (L2) was synthesized from 1 mmol of biphenyl-3,4,3',4'-tetraamine and 4 mmol of 2-furaldehyde dissolved in 15 mL of a nitrobenzene and the reaction mixture solution was refluxed at 90°C in an oil bath for 6 hrs

with continuous stirring. TLC was utilised to monitor the course of the reaction. After completion of 6 hrs, the reaction mixture was cooled and poured into the solvent hexane with continuous stirring. The raw product was completely purified by column chromatography and the major product was obtained as red solid. The yield was 80 % (Table 1)**.**

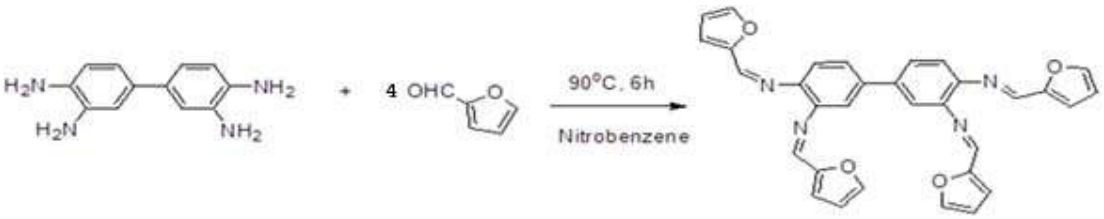

Biphenyl-3,4,3',4'-tetraamine

2- furaldehyde

(N3Z,N4Z,N3'Z,N4'E)-N3,N3',N4,N4'-tetrakis(furan-2-ylmethylene)-[1,1'-biphenyl]-3,3',4,4'-tetraamine [L2]

Scheme 2: Synthesis of N3Z, N4Z, N3'Z, N4'E)-N3, N3', N4, N4'-tetrakis(furan-2-ylmethylene)-[1,1'-biphenyl]-3,3',4,4'-tetraamine (L2) from biphenyl-3,4,3',4'-tetraamine and 2- furaldehyde.

Synthesis of Schiff base L3 from Biphenyl-3,4,3',4'-tetraamine and Indole -3-carboxyaldehyde

1 mmol of biphenyl-3,4,3',4'-tetraamine and 4 mmol of indole-3-carboxyaldehyde were dissolved in 15 mL of nitrobenzene and the reaction mixture was refluxed over an oil bath at 90^{o}C for 6 h with continuous stirring. TLC was utilised to monitor the progress of the reaction. After completion of 6 hrs, the reaction mixture was cooled and transferred into the solvent hexane with constant stirring. The raw product was completely purified with column chromatography and the required product (N3E, N4Z, N3'Z, N4'E)-N3, N3', N4, N4'-tetrakis((1H-indol-2-yl) methylene)-[1,1'-biphenyl]-3,3',4,4'-tetraamine) was obtained as reddish orange solid. Yield was 60%**.**

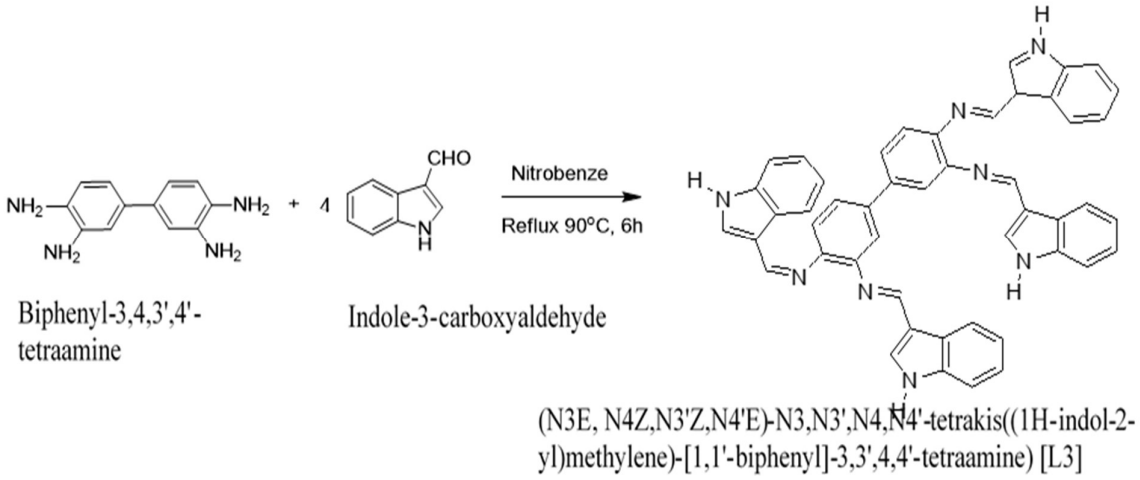

Scheme 3: Synthesis of N3E, N4Z, N3'Z, N4'E)-N3, N3', N4, N4'-tetrakis((1H-indol-2-yl) methylene)-[1,1'-biphenyl]-3,3',4,4'-tetraamine(L3) from biphenyl-3,4,3',4'-tetraamine and indole -3-carboxyaldehyde.

Solvents like nitro benzene, DMF, DMSO, THF, toluene, xylene, and ethanol were used for the synthesis of the compounds, L1, L2 and L3. It was observed that the solubility and purity of the compounds were excellent with the solvent, nitro benzene. But the compounds were insoluble in toluene and xylene. DMF and DMSO gave poor yield and selectivity. Work up problem with THF and ethanol.

Anti-cancer activity

MDA-MB-231 breast cancer cell lines were procured from the National Centre for Cell Sciences (NCCS), Pune, India. The cells were maintained in Dulbecco's Modified Eagle Medium (DMEM) supplemented with 10% fetal bovine serum (FBS) [36]. To prevent bacterial contamination, the medium was supplemented with penicillin (100 U/mL) and streptomycin (100 µg/mL). The cells were cultured in a humidified atmosphere containing 5% CO_2 at 37°C.

Cell cytotoxicity (MTT assay):

Cytotoxicity of compounds L1, L2, and L3 against MDA-MB-231 cells was assessed using Mosmann's assay *[37][38]*. For the cell viability assay, MDA-MB-231 cells were collected, and the number of viable cells were determined using a hemocytometer. The cells were diluted in DMEM media and seeded onto 96-well plates, with each well receiving 1×10^4 cells/ml. The plates were then incubated for 24 hours to facilitate adhesion. Following treatment of MDA-MB-231 cells with varying concentrations of L1, L2 and L3 (ranging from

5, 10, 15, 20, 25, and 30 μM/ml) were added to each well. For twenty-four hours, MDA-MB-231 cells were cultured at 37°C in a humidified environment with 95% air and 5% CO_2. Following incubation, the drug-containing cells were washed with fresh culture media, added MTT (5 mg/ml in PBS) dye to each well, and then allowed to incubate for an additional 4 hours at 37°C. A multi-well plate reader was utilised to measure the absorbance of purple precipitated formazan *[29][36]* formed, which was then dissolved in 100 μM of concentrated DMSO. This process was done to determine cell viability. In comparison to the control, the percentage of the stable cells were used to express the results. The optimal dosages were investigated at multiple time points, and the IC_{50} values were determined *[39]*.

The samples L1, L2, and L3 dose response curves, which show a 50% reduction in cytotoxicity when compared to vehicle control cells, were used to calculate the IC_{50} values. In triplicate, each experiment was run at least three times.

$$Inhibitory\ cell\ proliferation\ (\%) = \frac{[Mean\ absorbance\ of\ the\ control - Mea\quad absorbance\ of\ the\ sample]\ X\ 100}{Mean\ absorbance\ of\ the\ control}$$

Every experiment was conducted in at least three triplicates (T1, T2 and T3) in each study *[36]*.

Study of Apoptosis in treated cells using Acridine Orange and Ethidium Bromide

Measurement of apoptotic induction was done using acridine orange (AO) and ethidium bromide (EB). Apoptotic cell death was examined with a fluorescence microscope, according to Baskic et al. *[38]*. MDA-MB-231 cells were placed at a density of $5x10^4$ cells/well in a 6-well plate, and the cells were incubated for a full day. Following a 24-hour exposure to L1, L2, and L3 at 15, 20 and 25 μM/ml, the cells were separated, three PBS washes were run through them. The plates were stained for five minutes using a 1:1 ratio of acridine orange and ethidium bromide (100 μg/ml). Following this, they were examined right away at a 20x magnification using a fluorescence microscope. The proportion of cells displaying traits associated with apoptosis to the total number of cells in the field were determined.

Results and Discussion:

Characterization of N3Z, N4Z, N3'Z, N4'E)-N3, N3', N4, N4'-tetrakis(thiophen-2-ylmethylene)-[1,1'-biphenyl]-3,3',4,4'-tetraamine (L1):

^{1}H NMR (500 MHz, $CDCl_3$) δ (s, 1H) 5.72, (s, 1H) 5.96, (s, 1H) 6.02, (m, 3H) 6.92-6.96, (m, 2H) 7.03-7.04, (m, 3H) 7.22-7.24, (m, 2H) 7.37-7.39, (m, 2H) 7.60-7.62, (m, 4H) 7.72-7.79, (s, 1H) 7.83, (s, 1H) 7.93, (s, 1H) 8.03. (Figure S1)

^{13}C NMR (125 MHz, $CDCl_3$) δ (109.47, 111.59, 117.53, 119.73, 122.84, 123.28, 126.52, 126.65, 127.33, 127.37, 127.63, 128.42, 129.32, 129.38, 130.18, 130.26, 132.42, 132.58, 133.74, 134.21, 134.24, 135.68, 136.87, 137.00, 137.16, 139.84, 140.00, 142.23, 143.67, 147.76, 147.95, 148.20). (Figure S2)

IR: the spectrum was acquired with Agilent Resolutions Pro. The compound, L1, showed bands due to –C–S) stretching at 853-1090 cm^{-1} and (–N=C–) stretching, typical for a Schiff base, at 1614-1524 cm^{-1}, C–H stretching of aromatic at 3071 cm^{-1}, C=C stretching of aromatic ring at 1569-1367 cm^{-1}, C–H bending of aromatic at 829-493 cm^{-1}, C–N stretching at 1341-1231cm^{-1}. (Figure S3)

Mass spectrum- JEOL JMS DX-300 Mass Spectrometer was used for the determination of molecular weights. m/z molecular base peak – 591. (Figure S4)

Characterization of N3Z, N4Z, N3'Z, N4'E)-N3, N3', N4, N4'- tetrakis (furan-2-ylmethylene)-[1,1'-biphenyl]-3, 3', 4, 4'-tetraamine (L2):

^{1}H NMR (500 MHz, $CDCl_3$) δ 5.60-5.61 (d, 2H), 6.20-6.25 (m, 2H), 6.44-6.54 (m, 3H), 7.18-7.25 (m, 4H), 7.30 (s, 1H), 7.38 (s, 1H), 7.43 (s, 1H), 7.49-7.65 (m, 4H), 7.73-7.78 (m, 3H), 7.97 (s, 1H). (Figure S5)

^{13}C NMR (125 MHz, $CDCl_3$) – δ: 108.61, 108.70, 110.31, 110.61, 110.65, 110.85, 112.20, 112.33, 113.12, 113.29, 118.06, 119.70, 123.17, 123.33, 123.68, 134.78, 136.13, 137.06, 137.50, 142.12, 142.82, 142.86, 143.37, 143.84, 143.94, 144.15, 144.21, 144.73, 145.13, 145.25, 145.55, 149.47. (Figure S6)

IR The compound, L2 exhibited bands due to (C–O) stretching at 1300 cm^{-1}-1000 $cm^{-1}$and (N=C) stretching at 1650-1550 cm^{-1} (typical imine linkage of a Schiff base), C-H stretching

frequencies of aromatic at 3124 cm^{-1}, C=C stretching of aromatic ring at 1600-1300 cm^{-1}, C-H bending of aromatic at 880-638 cm^{-1}, C-N stretching at 1073 cm^{-1}, 1015 cm^{1},1226 cm^{1}. (Figure S7)

Mass spectrum – JEOL JMS DX-300 Mass Spectrometer was used for the determination of molecular weights. m/z molecular base peak – 527. (Figure S8)

Characterization of N3E, N4Z, N3'Z, N4'E)-N3, N3', N4, N4'-tetrakis((1H-indol-2-yl) methylene)-[1,1'-biphenyl]-3, 3', 4, 4'-tetraamine (L3):

^{1}H NMR (500 MHz, $CDCl_3$) δ (d, 2H) 5.80-5.87, (m, 8H) 6.83-7.43, (m, 9H) 7.44-8.11, (m, 7H) 8.18-8.48, (s, 1H) 10.68, (s, 1H) 10.93, (m, 3H) 11.54-11.60, (m, 3H) 12.35-12.43. (Figure S9)

IR Infrared (IR) spectrum was recorded on a Shimadzu infrared spectrophotometer using the KBr disc technique. The compound, L3 showed bands due to –C=N stretching at 1623 $cm^{-1}$and –N–H stretching of amine at 3404 cm^{-1}, C=C stretch of aromatic ring at 1573 cm^{-1}, 1455 cm^{-1}, C–N stretch at 1099 cm^{-1}, =C–C stretch at 805 cm^{-1}. (Figure S10)

Mass spectrum- JEOL JMS DX-300 Mass Spectrometer was used for the determination of molecular weights. m/z molecular base peak – 723. (Figure S11)

Based on the above results the structures of the compounds L1, L2 and L3, presented in the schemes 1-3, were derived. The studied compounds exhibit spectral characteristics in par with the literature data.

Anti-Cancer Activity

Cell Cytotoxicity: (MTT assay)

The viability of MDA-MB-231 at different concentrations of L1, L2, and L3 were listed in Table 2. A plot was generated by reporting the half-maximal inhibitory concentration (IC_{50}) and the determined percentage of cell viability or cytotoxicity against the different concentrations of L1, L2, and L3 (Figure 1). Using a fluorescent microscope, the viability and cytological properties of the MDA-MB-231 cells were assessed (Figure 2). The higher doses

of L1, L2, and L3 resulted in a considerable reduction in the number of viable MDA-MB-231 cells as well as structural disruption. *[36,40]*.

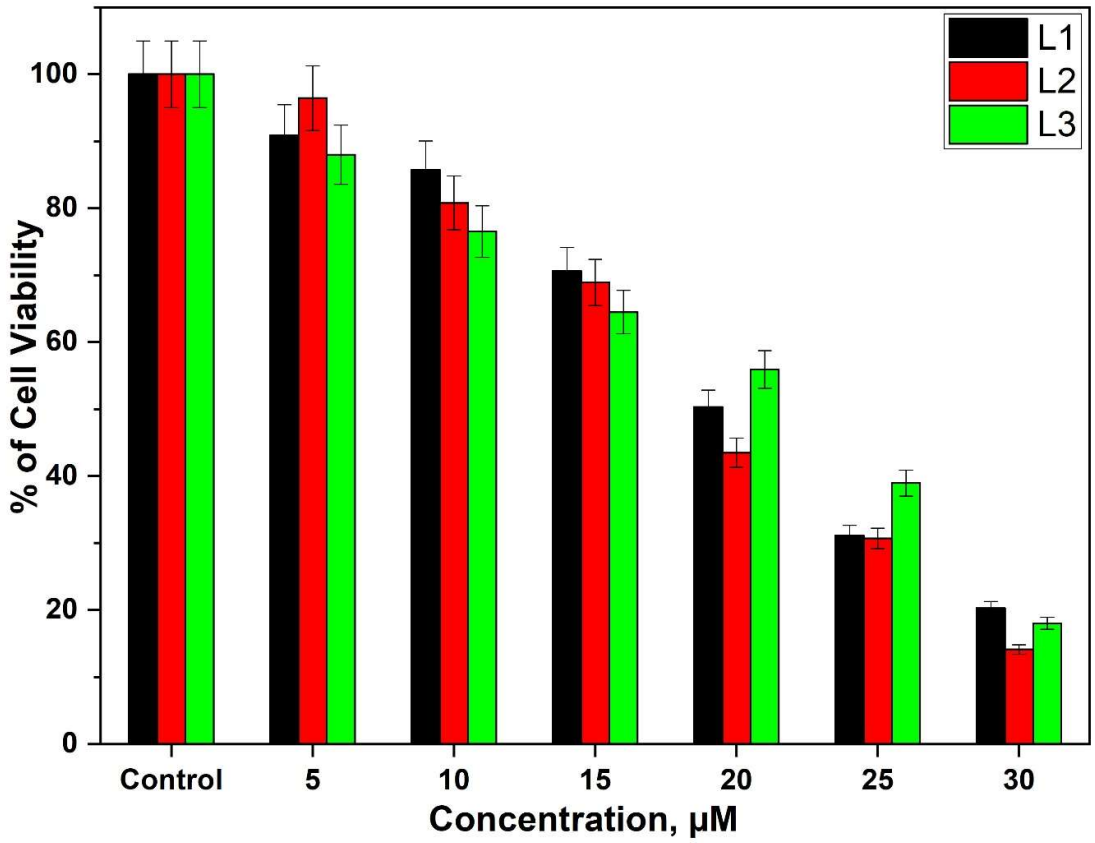

Figure 1 Effect of Compounds L1, L2, and L3 on Cell Viability determined by MTT Assay with MDA-MB-231 Cells.

Table 2: MTT Assay –MDA-MB-231 cell lines with L1, L2 and L3

	CONCENTRATION	Control	5 µM	10 µM	15 µM	20 µM	25 µM	30 µM
L1	T1	100	94.3299	89.69072	75.25773	55.15464	34.53608	24.74227
	T2	100	91.23711	85.56701	71.13402	50	30.92784	19.58763
	T3	100	87.1134	81.95876	65.46392	45.87629	27.83505	16.49485
	Average	100	90.89347	85.73883	70.61856	50.34364	31.09966	20.27492
	SD	0	3.620502	3.868843	4.91721	4.648711	3.353817	4.166444
L2	T1	100	98.30508	81.35593	70.62147	40.67797	30.50847	11.86441
	T2	100	93.22034	83.61582	72.31638	44.0678	26.55367	19.77401
	T3	100	97.74011	77.40113	63.84181	45.76271	35.02825	10.73446
	Average	100	96.42184	80.79096	68.92655	43.50283	30.6968	14.12429
	SD	0	2.786937	3.14563	4.484322	2.589023	4.240428	4.925309
L3	T1	100	84.69945	79.78142	68.85246	57.9235	35.51913	22.40437
	T2	100	88.52459	73.77049	61.20219	53.55191	41.53005	14.20765
	T3	100	90.71038	75.95628	63.38798	56.28415	39.89071	17.48634
	Average	100	87.97814	76.50273	64.48088	55.91985	38.97996	18.03279
	SD	0	3.042495	3.042495	3.940492	2.208446	3.107231	4.125592

When exposed to MDA-MB-231 cells at concentrations of 5, 10, 15, 20, 25, and 30 µM, the cell viability decreased as the concentration increased. The percentage of viability was observed as 91, 86, 71, 50, 31 & 20%, 96, 81, 69, 43, 31 & 14 % and 88, 76, 64, 56, 39 & 18 % with L1, L2 and L3 respectively. A 24-hour exposure resulted in a 50% reduction in cell viability[41]. The IC_{50} values of L1, L2 and L3 were estimated to be 20 µM/ml, 17µM/ml, and 22 µM/ml as a result of this discovery. Concentrations above 30 µM resulted in 100% cytotoxicity, with all cells being killed. Cells treated to 30µM/ml concentration of L1, L2 and L3 exhibited both a reduction in cell quantity and a change in shape [42].

Effect of L1, L2 and L3 on cell morphology:

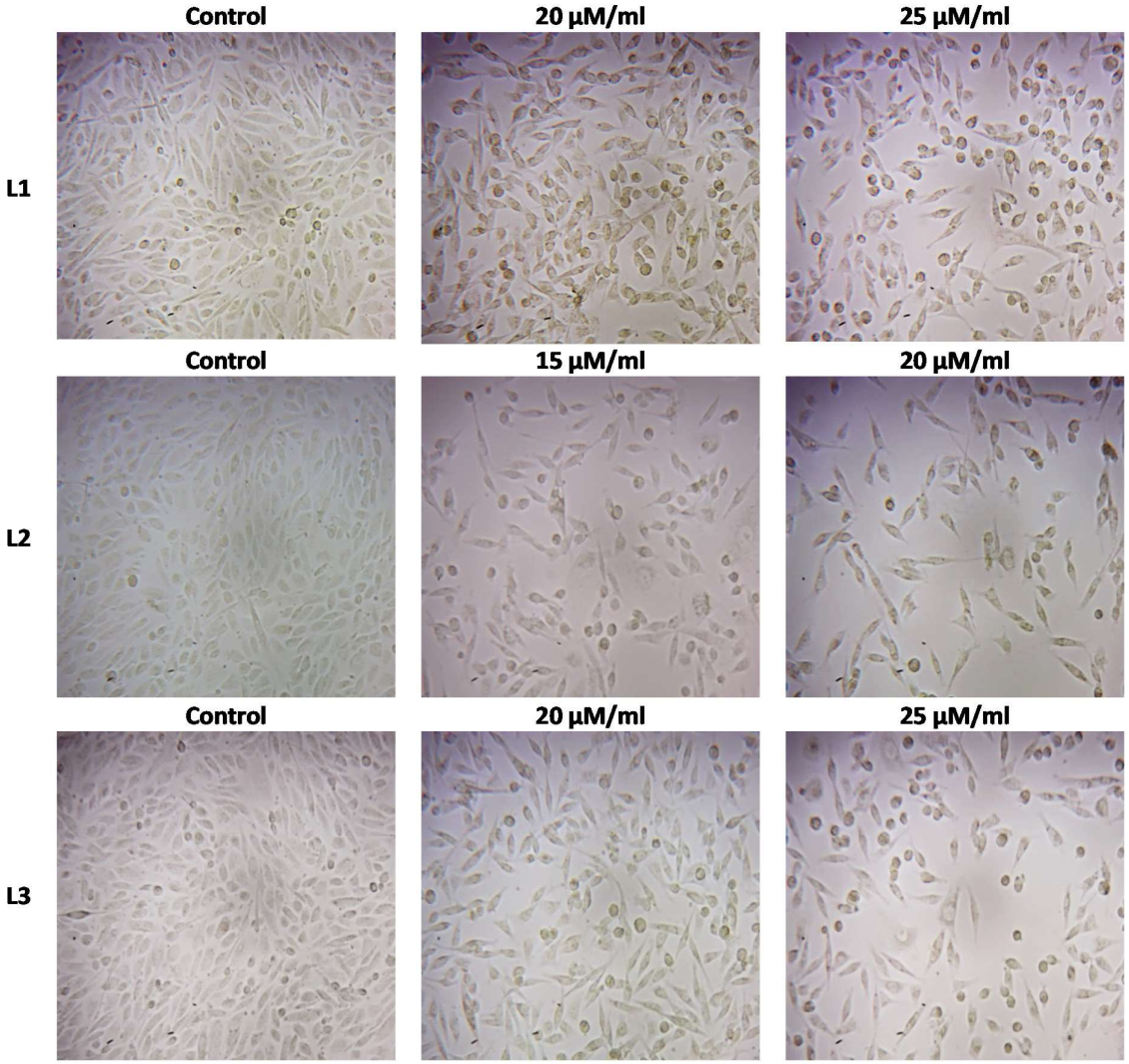

Figure 2 Changes in morphology in control and L1, L2 and L3 treated MDA-MB-231 cells for 24 h. A) control B)20µM/ml (L1, L3)15 µM/ml(L2) C) IC_{50}

Photomicrograph (20x) represents morphological changes in MDA-MB-231 cells such as shrinkage, detachment, membrane blebbing and distorted shape induced by sample in comparison to the control group after receiving treatment with L1 (20 and 25 µM/ml), L2 (15 and 20 µM/ml) and L3 (20 & 25 µM/ml) for 24 hours. Images of the control group were taken using a light microscope and revealed normal, intact cell morphology (Figure 2)*[36]*.

Apoptosis Induction in cells by L1, L2 and L3 stained with AO and EB:

After being exposed to L1 (20 and 25 µM), L2 (15 and 20 µM), and L3 (20 and 25 µM) for a whole day, human breast cancer cells were stained with dual dye AO and EB which were inspected with fluorescence microscope at a magnification of 20x[43].

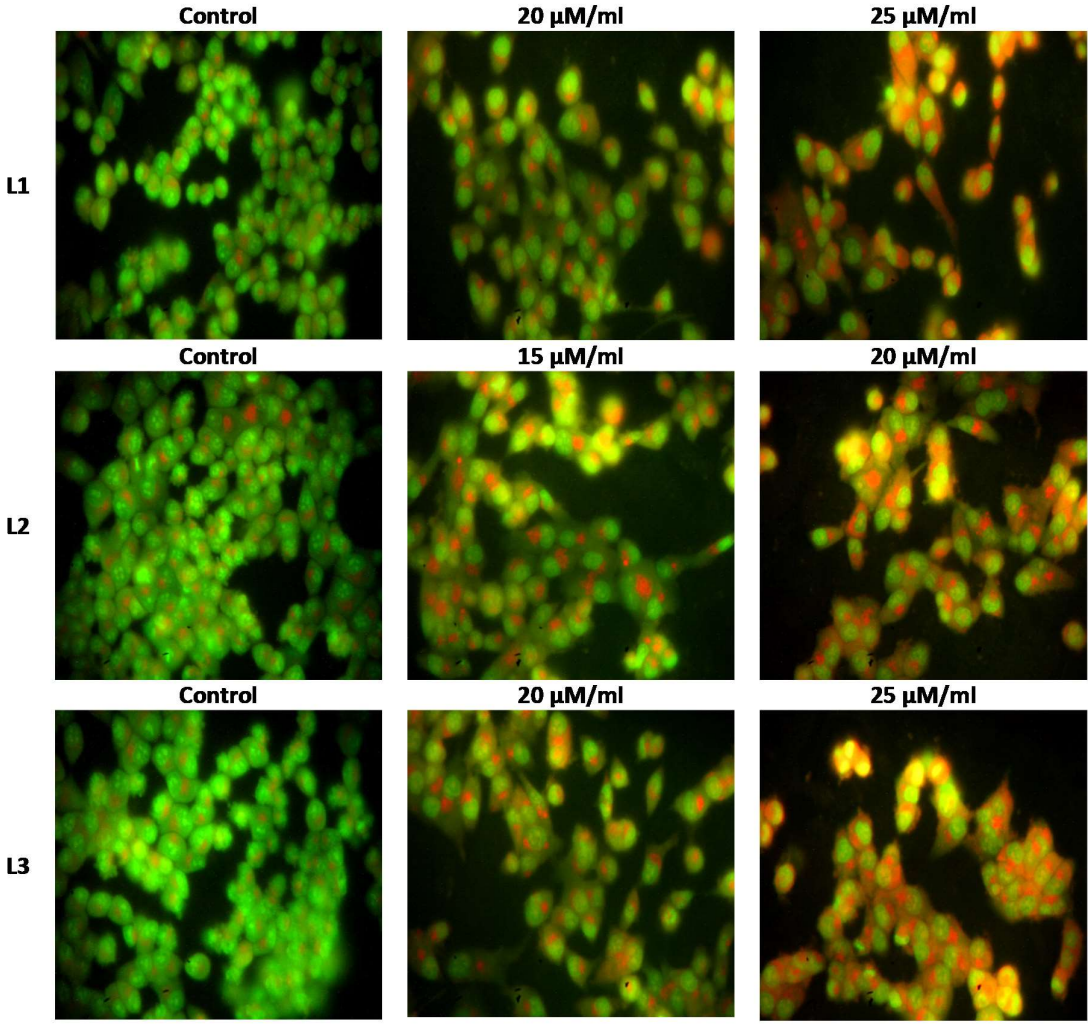

Figure 3: Acridine orange (AO) and ethidium bromide (EB) staining of L1, L2 and L3 of Control, 20 µM/ml(L1, L3)15 µM/ml (L2) and IC_{50} (last column).

Since AO is permeable, it can stain both viable and non-viable MDA-MB-231 cells. Upon intercalating into double-stranded DNA, it emits green fluorescence, whereas binding to single-stranded RNA results in red fluorescence. Only nonviable cells that have lost their membrane integrity can absorb EB, which then intercalates into DNA to produce red fluorescence.

Based on fluorescence emission and chromatin condensation morphology in labeled nuclei, they identified four distinct cell types. Viable cells exhibited regular nuclear structure

and intense green fluorescence. Early apoptotic cells showed green nuclei, indicating initial DNA cleavage, with peri-nuclear chromatin condensation appearing as bright green patches. Late apoptotic cells displayed orange to red nuclei with condensed or fragmented chromatin (Figure 3). In contrast, necrotic cells lacked condensed chromatin and consistently showed orange to red nuclei[44]. From Figure 3, Green fluorescence in the control cells denotes live cells devoid of apoptosis. The studied L1, L2, and L3 cells displayed yellow and orange fluorescence indicating condensed or fragmented early and late apoptotic cell death.

Acylpyrazolone-based Schiff base ligands (HL_n) and their corresponding Pt(II) complexes, [Pt(L_n)(Cl)] (n = 1–3) [45], demonstrated breast cancer activity against MDA-MB-231 cells, with the order of potency being [Pt(L1)Cl] > [Pt(L2)Cl] > [Pt(L3)Cl]. However, the biphenyl-3,4,3',4'-tetraamine-based Schiff bases, derived from 2-thiophene-2-carboxyaldehyde (L1), 2-furaldehyde (L2), and indole-3-carboxyaldehyde (L3), showed superior activity compared to the Acylpyrazolone-based Schiff base ligands. Notably, compounds L1, L2, and L3 exhibited excellent activity against MDA-MB-231 cell lines, with the order of potency being L2 > L1 > L3. The proposed aromatic tetramine-based Schiff bases offer a cost-effective alternative to aliphatic polyamines like spermine, with enhanced activity against resistant MDA-MB-231 cells.

Conclusions:

Well-characterized Schiff bases derived from 1,1'-biphenyl]-3,3',4,4'-tetraamine, with 2-thiophene carbaldehyde, 2-furaldehyde and indole-3-carbaldehyde, i.e., the compounds L1, L2, and L3 respectively were tested against breast cancer MDA-MB-231 cells. The compound L2 showed good inhibition of breast cancer cells followed by L1 and L3 (L2>L1>L3). The compounds, L1, L2 and L3 showed the IC_{50} values as 20 μM, 17 μM and 22 μM. From our results, we conclude that the compound, L2 is more effective as anti-cancer agent. Further research needs to be done to fully comprehend L2's mode of action and take this as a drug for the breast cancer cells to the next step.

Acknowledgement:

The authors are grateful to Late Dr. Ramesh Kumar, Department of Chemistry, Madras Christian College, Chennai for his continuous help for this study who passed away recently because of cardiac arrest. May his soul rest in peace.

References:

[1] The top 10 causes of death, (n.d.). https://www.who.int/news-room/fact-sheets/detail/the-top-10-causes-of-death (accessed August 26, 2024).

[2] Global cancer burden growing, amidst mounting need for services, (n.d.). https://www.who.int/news/item/01-02-2024-global-cancer-burden-growing--amidst-mounting-need-for-services (accessed June 26, 2024).

[3] Siegel, Rebecca L., Angela N. Giaquinto, and Ahmedin Jemal. "Cancer statistics, 2024." CA: a cancer journal for clinicians 74.1 (2024).

[4] K. Sathishkumar, M. Chaturvedi, P. Das, S. Stephen, P. Mathur, Cancer incidence estimates for 2022 & projection for 2025: Result from National Cancer Registry Programme, India, Indian J Med Res 156 (2022) 598. https://doi.org/10.4103/IJMR.IJMR_1821_22.

[5] R.A. Lambert, Comparative Studies Upon Cancer Cells and Normal Cells: Ii. The Character of Growth In Vitro With Special Reference to Cell Division, J Exp Med 17 (1913) 499–510.

[6] S.A. Godinho, M. Kwon, D. Pellman, Centrosomes and cancer: How cancer cells divide with too many centrosomes, Cancer and Metastasis Reviews 28 (2009) 85–98. https://doi.org/10.1007/S10555-008-9163-6/METRICS.

[7] U. Anand, A. Dey, A.K. Singh Chandel, R. Sanyal, A. Mishra, D.K. Pandey, V. De Falco, A. Upadhyay, R. Kandimalla, A. Chaudhary, J.K. Dhanjal, S. Dewanjee, J. Vallamkondu, J.M. Pérez De La Lastra, Cancer chemotherapy and beyond: Current status, drug candidates, associated risks and progress in targeted therapeutics, (n.d.). https://doi.org/10.1016/j.gendis.2022.02.007.

[8] G. Mathur, S. Nain, P.K. Sharma, Cancer: An Overview, Academic Journal of Cancer Research 8 (2015) 1–09. https://doi.org/10.5829/idosi.ajcr.2015.8.1.9336.

[9] S. Di Meo, P. Venditti, Evolution of the Knowledge of Free Radicals and Other Oxidants, Oxid Med Cell Longev 2020 (2020). https://doi.org/10.1155/2020/9829176.

[10] J.R. Benson, I. Jatoi, The global breast cancer burden, Future Oncol 8 (2012) 697–702. https://doi.org/10.2217/FON.12.61.

[11] M. Zendehdel, B. Niakan, A. Keshtkar, E. Rafiei, F. Salamat, A Systematic Review and Meta-Analysis Protocol, Iran J Med Sci 43 (2018) 1–8.

[12] P. Alexandra, S. Veiga, Oncology and Infectious Diseases in Ancient Egypt: The Ebers Papyrus' Treatise on Tumours 857-877 and the Cases Found in Ancient Egyptian Human Material, (2009). http://hdl.handle.net/10919/71527 (accessed September 17, 2024).

[13] A.R. David, M.R. Zimmerman, Cancer: an old disease, a new disease or something in between?, Nature Reviews Cancer 2010 10:10 10 (2010) 728–733. https://doi.org/10.1038/nrc2914.

[14] R.L. Siegel Mph, K.D. Miller, N. Sandeep, W. Mbbs, | Ahmedin, J. Dvm, R.L. Siegel, Cancer statistics, 2023, CA Cancer J Clin 73 (2023) 17–48. https://doi.org/10.3322/CAAC.21763.

[15] Breast cancer, (n.d.). https://www.who.int/news-room/fact-sheets/detail/breast-cancer (accessed March 4, 2024).

[16] Y. Vargas Casanova, J.A. Rodríguez Guerra, Y.A. Umaña Pérez, A.L. Leal Castro, G. Almanzar Reina, J.E. García Castañeda, Z.J. Rivera Monroy, Antibacterial Synthetic Peptides Derived from Bovine Lactoferricin Exhibit Cytotoxic Effect against MDA-MB-468 and MDA-MB-231 Breast Cancer Cell Lines, Molecules 22 (2017). https://doi.org/10.3390/MOLECULES22101641.

[17] A. Satija, S.M. Ahmed, R. Gupta, A. Ahmed, S.P.S. Rana, S.P. Singh, S. Mishra, S. Bhatnagar, Breast cancer pain management - A review of current & novel therapies, Indian J Med Res 139 (2014) 216. /pmc/articles/PMC4001332/ (accessed December 24, 2023).

[18] Hormone Therapy for Breast Cancer | Breast Cancer Treatment | American Cancer Society, (n.d.). https://www.cancer.org/cancer/types/breast-cancer/treatment/hormone-therapy-for-breast-cancer.html (accessed November 12, 2023).

[19] J. Siglin, C.E. Champ, Y. Vakhnenko, P.R. Anne, N.L. Simone, Radiation Therapy for Locally Recurrent Breast Cancer, Int J Breast Cancer 2012 (2012). https://doi.org/10.1155/2012/571946.

[20] W.M. Eldehna, D.H. El-Naggar, A.R. Hamed, H.S. Ibrahim, H.A. Ghabbour, H.A. Abdel-Aziz, One-pot three-component synthesis of novel spirooxindoles with potential

cytotoxic activity against triple-negative breast cancer MDA-MB-231 cells, J Enzyme Inhib Med Chem 33 (2018) 309–318. https://doi.org/10.1080/14756366.2017.1417276.

[21] K. Zibara, Z. Awada, L. Dib, J. El-Saghir, S. Al-Ghadban, A. Ibrik, N. El-Zein, M. El-Sabban, Anti-angiogenesis therapy and gap junction inhibition reduce MDA-MB-231 breast cancer cell invasion and metastasis in vitro and in vivo, Scientific Reports 2015 5:1 5 (2015) 1–16. https://doi.org/10.1038/srep12598.

[22] U. Bachrach, The early history of polyamine research, Plant Physiol Biochem 48 (2010) 490–495. https://doi.org/10.1016/J.PLAPHY.2010.02.003.

[23] H.M. Wallace, A. V. Fraser, A. Hughes, A perspective of polyamine metabolism, Biochem J 376 (2003) 1–14. https://doi.org/10.1042/BJ20031327.

[24] L.J. Marton, A.E. Pegg, Polyamines as targets for therapeutic intervention, Annu Rev Pharmacol Toxicol 35 (1995) 55–91. https://doi.org/10.1146/ANNUREV.PA.35.040195.000415.

[25] T.J. Carneiro, R. Araújo, M. Vojtek, S. Gonçalves-monteiro, A.L.M. Batista de Carvalho, M.P.M. Marques, C. Diniz, A.M. Gil, Impact of the pd2spm (Spermine) complex on the metabolism of triple-negative breast cancer tumors of a xenograft mouse model, Int J Mol Sci 22 (2021) 10775. https://doi.org/10.3390/IJMS221910775/S1.

[26] A.M. Asiri, S.A. Khan, H.M. Marwani, K. Sharma, Synthesis, spectroscopic and physicochemical investigations of environmentally benign heterocyclic Schiff base derivatives as antibacterial agents on the bases of in vitro and density functional theory, J Photochem Photobiol B 120 (2013) 82–89. https://doi.org/10.1016/J.JPHOTOBIOL.2013.01.007.

[27] C. Sci, D. Chaturvedi, M. Kamboj, Role of Schiff Base in Drug Discovery Research, Chem Sci J 7 (2016) 114. https://doi.org/10.4172/2150-3494.1000e114.

[28] A. Kajal, S. Bala, S. Kamboj, N. Sharma, V. Saini, Schiff Bases: A Versatile Pharmacophore, Journal of Catalysts 2013 (2013) 1–14. https://doi.org/10.1155/2013/893512.

[29] Hemalatha, G. M., Thirunavukkarasu, K. A. N. D. A. S. A. M. Y., & Kumar, C. R. (2022). Isoniazid-based schiffs bases in bone cancer studies using MG-63 cell lines. Int J App Pharm, 14, 168-74.

[30] M.A. Malik, O.A. Dar, P. Gull, M.Y. Wani, A.A. Hashmi, Heterocyclic Schiff base transition metal complexes in antimicrobial and anticancer chemotherapy, Medchemcomm 9 (2017) 409–436. https://doi.org/10.1039/C7MD00526A.

[31] Hemalatha, G. M., Thirunavukkarasu, K., Kumar, C. R., Thamim, M., & Thirumoorthy, K. (2023). Selective Detection of Copper Ions and Biological Activities of Isoniazid Schiff Bases. ChemistrySelect, 8(12), e202204898.

[32] F.K. Ommenya, E.A. Nyawade, D.M. Andala, J. Kinyua, Synthesis, Characterization and Antibacterial Activity of Schiff Base, 4-Chloro-2-{(E)-[(4-Fluorophenyl)imino]methyl}phenol Metal (II) Complexes, J Chem 2020 (2020). https://doi.org/10.1155/2020/1745236.

[33] W. Al Zoubi, W. Al Zoubi, Biological Activities of Schiff Bases and Their Complexes: A Review of Recent Works, Int J Org Chem (Irvine) 3 (2013) 73–95. https://doi.org/10.4236/IJOC.2013.33A008.

[34] J. Ceramella, D. Iacopetta, A. Catalano, F. Cirillo, R. Lappano, M.S. Sinicropi, A Review on the Antimicrobial Activity of Schiff Bases: Data Collection and Recent Studies, Antibiotics 2022, Vol. 11, Page 191 11 (2022) 191. https://doi.org/10.3390/ANTIBIOTICS11020191.

[35] Khan, E., Hanif, M., & Akhtar, M. S. (2022). Schiff bases and their metal complexes with biologically compatible metal ions; biological importance, recent trends and future hopes. Reviews in Inorganic Chemistry, 42(4), 307-325.

[36] M. Vijayapriya, S. Mahalakshmi, C.R. Christiya, In-Vitrostudies on Antiproliferative Effect of Euphorbiahirta L Leaves, Ann Rom Soc Cell Biol 25 (2021) 11111–11126. https://www.annalsofrscb.ro/index.php/journal/article/view/3891 (accessed December 24, 2023).

[37] T. Mosmann, Rapid colorimetric assay for cellular growth and survival: application to proliferation and cytotoxicity assays, J Immunol Methods 65 (1983) 55–63. https://doi.org/10.1016/0022-1759(83)90303-4.

[38] D. Baskić, S. Popović, P. Ristić, N.N. Arsenijević, Analysis of cycloheximide-induced apoptosis in human leukocytes: fluorescence microscopy using annexin V/propidium

iodide versus acridin orange/ethidium bromide., Cell Biol Int 30 (2006) 924–932. https://doi.org/10.1016/J.CELLBI.2006.06.016.

[39] S. Mohanasundaram, N. Rangarajan, V. Sampath, K. Porkodi, M. Pennarasi, GC–MS and HPLC analysis of antiglycogenolytic and glycogenic compounds in kaempferol 3–O–gentiobioside containing Senna alata L leaves in experimental rats, Translational Metabolic Syndrome Research 4 (2021) 10–17. https://doi.org/10.1016/J.TMSR.2021.07.001.

[40] P. Suresh, A.S. Xavier, V.P. Karthik, K. Punnagai, Anticancer activity of cissus quadrangularis l. Methanolic extract against MG63 Human osteosarcoma cells – an in-vitro evaluation using cytotoxicity assay, Biomedical and Pharmacology Journal 12 (2019) 975–980. https://doi.org/10.13005/BPJ/1724.

[41] D. Hopkinson, R. Bourne, D.A. Barile, In Vitro Cytotoxicity Testing: 24-hour and 72-hour Studies with Cultured Lung Cells, Alternatives to Laboratory Animals 21 (1993) 167–172. https://doi.org/10.1177/026119299302100208.

[42] J. Folkman, A. Moscona, Role of cell shape in growth control, Nature 1978 273:5661 273 (1978) 345–349. https://doi.org/10.1038/273345a0.

[43] K. Liu, P. cheng Liu, R. Liu, X. Wu, Dual AO/EB Staining to Detect Apoptosis in Osteosarcoma Cells Compared with Flow Cytometry, Med Sci Monit Basic Res 21 (2015) 15. https://doi.org/10.12659/MSMBR.893327.

[44] M.E. Bianchi, A. Manfredi, Chromatin and cell death, Biochimica et Biophysica Acta (BBA)- Gene Structure and Expression 1677 (2004) 181–186. https://doi.org/10.1016/J.BBAEXP.2003.10.017.

[45] Eslami Moghadam, M., Hasanzadeh Esfahani, M., Behzad, M., Zolghadri, S., Ramezani, N., & Azadi, Y. (2023). New platinum (II) complexes based on Schiff bases: synthesis, specification, X-ray structure, ADMET, DFT, molecular docking, and anticancer activity against breast cancer. JBIC Journal of Biological Inorganic Chemistry, 28(5), 519-529.